

Doppler-free Rb saturation spectroscopy

Florian Jung

May 3rd, 2018

supervisor: Dr. Christian Chmelik

Contents

1	Introduction and basics	3
2	Natural line width and mechanisms of line broadening	5
2.1	Natural line width	5
2.2	Doppler broadening	7
2.3	Homogeneous and inhomogeneous line broadening	10
2.4	Optical pumping	10
2.5	Saturation broadening of homogeneously broadened transitions	11
2.6	Linear and nonlinear absorption	13
2.7	Saturation broadening of inhomogeneously broadened transitions	15
3	Origin of fine structure and hyperfine structure	18
3.1	Fine structure	18
3.2	Hyperfine structure	18
4	Structure of a laser diode	20
4.1	Introduction to semiconductors	20
4.2	Doping of semiconductors	22
4.3	p-n junction without external voltage	24
4.4	p-n junction with external voltage	25
4.5	Laser diode	25
4.5.1	Basics and laser conditions	25
4.5.2	Realizations	29
4.5.3	Tuning the laser diode	29
5	Set-up of a Fabry-Pérot interferometer (FPI)	30
6	Saturation spectroscopy	33
7	Experimental procedure and list of tasks	34

1 Introduction and basics

Laser spectroscopy allows to gain insights into different energy levels in atoms, molecules or even solids. In classical laser absorption spectroscopy, the absorption of a nearly monochromatic laser beam of known intensity by the material under study is considered. For example, with tunable lasers it is possible to scan through different frequencies of the electromagnetic spectrum and thus obtain information about the energy differences between transitions in the investigated substance.

Those energies in which absorption maxima are observable in the spectrum are called resonance frequencies. Due to the Heisenberg uncertainty principle, the line shape of these transitions is not a sharp line, but follows a Lorentzian distribution. The width of the Lorentz curve at half of the maximum intensity (FWHM) that would be observable at $T = 0$ K is called the natural line width. The physical meaning is again related with the Heisenberg uncertainty principle. Since energy (and thus frequency) and time are conjugate quantities, the natural line width $\tau \propto \frac{1}{E}$ is a measure of the lifetime of an excited state. In the following, the spectroscopy of gases shall be considered.

If one considers a gas with one type of molecules at a temperature $T > 0$ K, one finds that the individual molecules have different velocities with a distribution following Maxwell-Boltzmann statistics. Because of this movement, not the energies ω in the laser are absorbed by the gas, which correspond to the molecular transitions $\omega_{0,i}$, but those with Doppler shifted frequencies $\omega'_{0,i} = \omega_{0,i} - \vec{v} \cdot \vec{k}$ (with \vec{k} as the wave vector of the absorbed radiation and \vec{v} as velocity of the molecules; ω' : velocity measured in the rest frame of the moving molecule). This effect leads to a so-called Doppler broadening of the line shape, which is several orders of magnitude higher than the natural line width. The basics of natural line width and various broadening mechanisms are presented in chapter 2.

In order to estimate the lifetime of excited states or to resolve hyperfine components (discussed in more detail in chapter 3), a spectroscopy method is required that allows to eliminate the effects of Doppler broadening. One such method is the Doppler-free saturation spectroscopy, which shall be the subject of this lab experiment.

The basic idea of this spectroscopy technique is very simple. The following components are needed: a tunable laser, a gas cell (usually contains a gas of alkali metals), various optical elements for adjusting the optical path and attenuation of the laser intensity, a Fabry-Perot interferometer (detailed explanation can be found in chapter 5) for setting the emission frequency of the laser diode and a photodiode for recording the intensity of the laser light after passing through the gas cell.

By a beam splitter and highly reflecting mirrors, the laser beam is split into two parts: the first being unattenuated or with low attenuation and shorter optical path goes in one direction through the gas cell and the second with substantial attenuation, passes

the gas cell in the reverse direction. The intensity ratio should be about one order of magnitude. The only slightly attenuated beam is referred to as "pump beam" and causes a population inversion by exciting transitions of matching energy. Therefore, the strongly attenuated beam ("probe beam") can pass nearly unhindered and is only weakly absorbed.

Now, let us consider a two-level system. If the frequency of the laser radiation is below the absorption frequency of the transition between the levels of the non-moving (!) molecule, the light of the pump beam is absorbed by molecules moving opposite to the pump beam \vec{k} while the light of the probe beam is absorbed by molecules that move opposite to the probe beam.

However, if the frequency of the laser light just matches the transition in non-moving molecules, the light of the pumping beam is absorbed only by atoms that are stagnant or moving perpendicular to the propagation direction of the laser light. Again, the probe beam is only weakly absorbed. Instead, so-called "lamb dips" are formed in the line profile. The difference between spectra with absorption from only one beam and the probe beam with opposed saturation beam then yields the "Doppler-corrected" lines.

In the following, the theoretical basics for understanding the experiment will be explained. Furthermore, a detailed structure of this lab experiment is presented in chapter 7.

2 Natural line width and mechanisms of line broadening

The explanations and calculations in this section closely follow [1]. Some of the calculations are shown with more intermediate steps here. However, a variety of useful additional information can and should be read in [1].

2.1 Natural line width

In an atom, there are various discrete energy levels whose distance is characteristic for the particular element or molecule. Without external influences, a molecule is in the so-called *ground state*. A transition to excited states may occur by various mechanisms, e.g. by collisions with other excited molecules or by absorption of electromagnetic radiation of appropriate wavelength. The excited levels are usually not stable; instead, within the so-called relaxation time τ_{rel} , the transition of the molecule to the ground state or other intermediate states takes place.

Molecules in an excited state can be described by a harmonic oscillation and the energy loss by radiation by an attenuation of this oscillation. The universal oscillator equation of this process is given by:

$$m\ddot{x} + \gamma\dot{x} + \omega_0^2x = 0 \quad (1)$$

In this equation $\omega_0^2 = \frac{k}{m}$ with k as spring constant of the oscillation and m the mass of the excited electron. γ is the decay constant of the vibration. The general solution with initial conditions $x(0) = x_0, \dot{x} = 0$ results in:

$$x(t) = x_0e^{-\frac{\gamma}{2}t} \left(\cos(\omega t) + \frac{\gamma}{2\omega} \sin(\omega t) \right) \quad (2)$$

Here is $\omega = \sqrt{\omega_0^2 - \frac{\gamma^2}{4}}$. Usually, the damping constant is $\gamma \ll \omega_0$, so it can be assumed that $\omega \approx \omega_0$ and $\frac{\gamma}{2\omega} \ll 1$. The sine dependence in $x(t)$ can thus be neglected. The damping constant conditions a harmonic oscillation that decays exponentially in time, as shown in figure 1. Since $x(t)$ is a periodic function, it can be written as a sum of various Fourier components representing frequency components $F(\omega)$ of the oscillation. It results to

$$x(t) = \frac{1}{\sqrt{2\pi}} \int_0^\infty F(\omega) e^{i\omega t} d\omega \quad (3)$$

The prefactor $\frac{1}{\sqrt{2\pi}}$ is a convention, however the product of the prefactors of a periodic function and its Fourier transform should always result to $\frac{1}{2\pi}$. Important for further consideration is the explicit form of the $F(\omega)$, as its square of the absolute value corresponds to the intensity of the radiated radiation – a quantity which is experimentally accessible. They are obtained by inverse Fourier transformation of $x(t)$, i.e.:

$$F(\omega) = \frac{1}{\sqrt{2\pi}} \int_{-\infty}^\infty x(t) e^{-i\omega t} dt = \frac{1}{\sqrt{2\pi}} \int_0^\infty x_0 e^{-\frac{\gamma}{2}t} \cos(\omega_0 t) e^{-i\omega t} dt \quad (4)$$

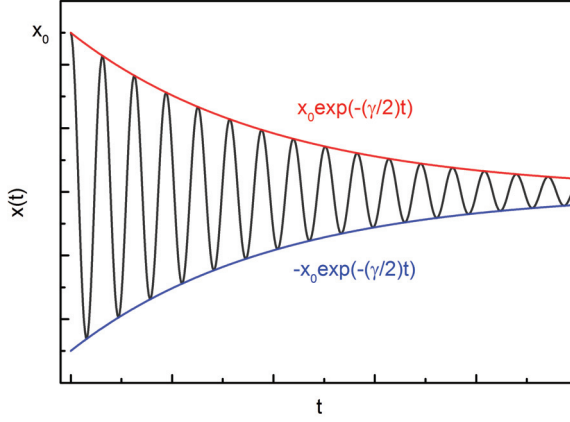


Figure 1: Representation of a damped oscillation, as occurring during the transition of a molecule from an excited to the ground state.

In the second step, it was implied that the transition is temporary and its beginning can be set arbitrarily. Integration for $t \in (-\infty, 0)$ vanishes because of $x(t) = 0$ for $t < 0$. A calculation of the intensity distribution by evaluating the analytically solvable integral in the region of ω_0 yields:

$$I(\omega - \omega_0) = A(\omega - \omega_0)A^*(\omega - \omega_0) \propto \frac{1}{(\omega - \omega_0)^2 + (\frac{\gamma}{2})^2} \quad (5)$$

To calculate the constant of proportionality, the intensity distribution needs to be normalized. This way the integral total intensity becomes equal to a constant I_0 .

$$\int_{-\infty}^{\infty} I(\omega - \omega_0)d(\omega - \omega_0) \simeq \int_0^{\infty} I(\omega)d\omega = \int_0^{\infty} \frac{K}{\omega^2 + (\frac{\gamma}{2})^2}d\omega \quad (6)$$

$$= \left(\frac{\gamma}{2}\right)^2 K \int_0^{\infty} \frac{1}{\left(\frac{2\omega}{\gamma}\right)^2 + 1}d\omega \quad (7)$$

By substituting $\Omega = \frac{2\omega}{\gamma}$ and, hence, $d\omega = \frac{\gamma}{2}d\Omega$ with $\int \frac{1}{1+x^2}dx = \arctan(x)$ it follows:

$$K = \frac{I_0\gamma}{2\pi} \quad (8)$$

By normalizing the previously described line profile for $I(\omega)$ with this intensity I_0 , one obtains the intensity profile:

$$g(\omega) = \frac{\frac{\gamma}{2\pi}}{(\omega - \omega_0)^2 + (\frac{\gamma}{2})^2} \quad (9)$$

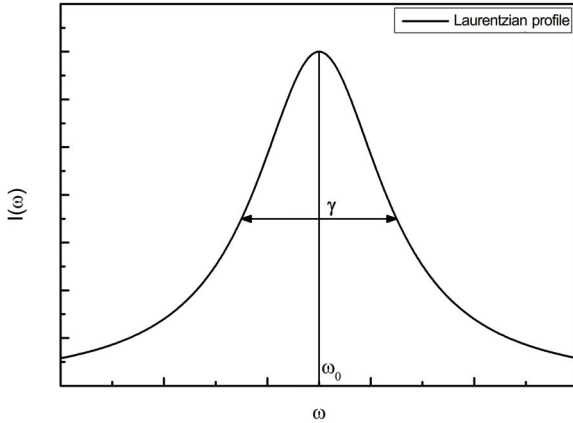


Figure 2: The profile of a Lorentzian distribution with center frequency ω_0 and FWHM γ .

This profile is called *Lorentzian profile* (see figure 2) and its full width at half maximum (FWHM) is called natural line width $\delta\omega_n$. With $g(\omega_0) = \frac{\gamma}{2\pi} \left(\frac{2}{\gamma}\right)^2 = \frac{2}{\gamma\pi}$ and thus $g\left(\omega_0 + \frac{\delta\omega_n}{2}\right) = \frac{1}{\gamma\pi}$ one obtains $\delta\omega_n = \gamma$. Using the Heisenberg uncertainty relation $\Delta E \Delta \tau > \hbar$ this natural line width can be correlated with the lifetime of the excited state via $\frac{\delta\omega_n}{2\pi} = \frac{1}{\tau}$. The *life time* of the state is the time after which the emitted intensity has dropped to $\frac{1}{e}$ of its initial value.

Just to mention one example, taken from [1]: The natural line width of the sodium D-line (transition from $3^2P_{1/2}$ to $3^2S_{1/2}$ within $\tau = 16$ ns) is 10 MHz.

Thus, from measurements of the natural line width of a state one can directly calculate the lifetime of this state. However, in practice the natural line width is increased substantially due to a variety of processes, such as Doppler or impact broadening. Thus, methods that compensate for broadening effects are needed in order to reveal information about the atomic or molecular structure of the investigated substances. Aim of this experiment is to introduce to such a method.

The following section deals with the broadening of lines by the effect of Doppler broadening.

2.2 Doppler broadening

Real spectroscopic measurements are rarely performed near absolute zero, but usually at higher temperatures. Due to the thermal energy the particles in a gas are in constant motion. The velocities of the individual particles of the gas obey a Maxwell velocity-distribution. A non-moving molecule shall emit light with frequency ω_0 . If it moves with a speed of \vec{v} with respect to a non-moving observer, for the observer the frequency

would shift to $\omega = \omega_0 + \vec{k} \cdot \vec{v}$. If the coordinate system is oriented in such a way that the x -direction coincides with the propagation direction of the wave, then this expression is simplified to:

$$\omega = \omega_0 + k_x v_x = \omega_0 \left(1 + \frac{v_x}{c} \right) \quad (10)$$

If the gas is treated as an ideal gas, the probability that a particle state is occupied is proportional to $e^{\frac{-mv^2}{2k_B T}}$. If, further, a constant density of states in the velocity space is assumed, all states of equal energy fall into the velocity interval $v + dv$ on a spherical surface $4\pi v^2$. The probability distribution of the velocities thus results to:

$$p(v)dv = k4\pi v^2 e^{\frac{-mv^2}{2k_B T}} dv \quad (11)$$

By normalizing $\int_0^\infty p(v)dv \stackrel{!}{=} 1$ one obtains $k = \left(\frac{m}{2k_B T \pi}\right)^{\frac{3}{2}}$ and it follows for the Maxwell-Boltzmann distribution

$$p(v)dv = 4\pi \left(\frac{m}{2k_B T \pi}\right)^{\frac{3}{2}} v^2 e^{\frac{-mv^2}{2k_B T}} dv \quad (12)$$

From $\frac{\partial p(v)}{\partial v} \stackrel{!}{=} 0$ the most probable speed is calculated to $e^{\frac{-mv^2}{2k_B T}}$.

Considering only one velocity component, for example v_x , under the same conditions as above the distribution function is given by:

$$p(v_x)dv_x = \sqrt{\frac{m}{2k_B T \pi}} e^{\frac{-mv_x^2}{2k_B T}} dv_x = \frac{1}{v_p \sqrt{\pi}} e^{-\left(\frac{v_x}{v_p}\right)^2} dv_x \quad (13)$$

In the last step, the most probable velocity v_p as calculated above was inserted. This velocity distribution can now be linked to the density $n_i(v_x)$ of the absorbing or emitting atoms or molecules in a state $|i\rangle$:

$$n_i(v_x)dv_x = N_i \frac{1}{v_p \sqrt{\pi}} e^{-\left(\frac{v_x}{v_p}\right)^2} dv_x \quad (14)$$

N_i represents the total number of molecules in state $|i\rangle$ per unit volume. In general, the velocities of the molecules and atoms can not be measured directly. However, spectroscopic measurements grant access to the distribution as a function of the absorption or emission frequencies and (14) can be rewritten using (10). First we calculate $v_x = c \frac{\omega - \omega_0}{\omega_0}$ and, furthermore, $dv_x = c \frac{1}{\omega_0} d\omega$ and it results for the density distribution $n_i(\omega)$:

$$n_i(\omega)d\omega = \frac{N_i}{v_p \sqrt{\pi}} \frac{c}{\omega_0} e^{-c^2 \left(\frac{\omega - \omega_0}{v_p \omega_0}\right)^2} d\omega \quad (15)$$

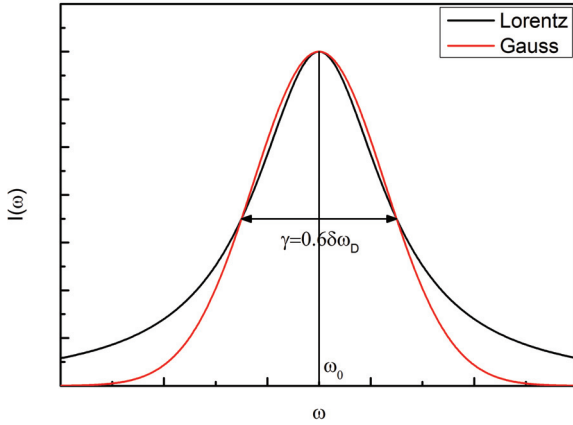


Figure 3: Comparison of a Gaussian and a Lorentzian profile with similar maximum value, center frequency and line width.

Since the intensity distribution $I(\omega)$ is proportional to the density distribution function $n_i(\omega)$, it can be written as:

$$I(\omega) = I(\omega_0) e^{-\left(\frac{\omega-\omega_0}{\omega_0 v_p/c}\right)^2} \quad (16)$$

This represents a *Gaussian distribution*. A comparison of a Lorentzian and a Gaussian profile is shown in figure 3. The FWHM, which represents an important spectroscopic parameter, can now be calculated analogously to the procedure for the natural line width and results to:

$$\text{FWHM}_D = \delta\omega_D = \sqrt{\frac{\omega_0^2 8k_B T \ln(2)}{mc^2}} = \sqrt{\frac{\omega_0^2 8RT \ln(2)}{Mc^2}} \quad (17)$$

Here M is the molar mass of the considered atoms or molecules. The Doppler width thus scales linearly with the considered center frequency ω_0 , $\propto \sqrt{T}$ and $\propto \sqrt{\frac{1}{m}}$ or $\propto \sqrt{\frac{1}{M}}$, respectively. The Doppler width of the Na line considered as example in the section 2.1 is $\delta\nu_D \approx 1,7\text{GHz}$, which is two orders of magnitude higher than the natural line width! According to the discussion above, each radiating transition in the Doppler-Gaussian profile has a Lorentzian profile at the different frequencies ω' . Thus, the profile ultimately results in a convolution of a Lorentzian and a Gaussian profile:

$$I(\omega - \omega') = I_0 \int (\omega - \omega') n(v_x) dv_x \quad (18)$$

This type of profile is called *Voigt profile*. In figure 4 a Voigt, a Gaussian and a Lorentzian profile are shown in comparison, which agree in important spectroscopic parameters. In

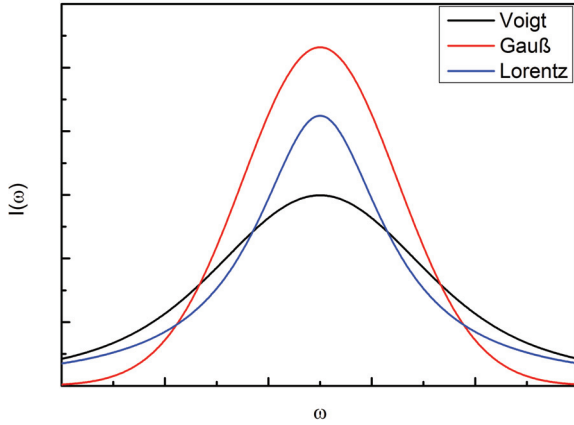


Figure 4: Comparison of a Voigt, a Gaussian and a Lorentzian profile with the same half width, center frequency and area.

some cases it is legitimate to consider a so-called "Pseudo-Voigt distribution" instead of a Voigt distribution, which results from the weighted sum of a Lorentzian and Gaussian profile rather than a convolution. Such a procedure is described for example in [2].

2.3 Homogeneous and inhomogeneous line broadening

A spectral profile of a transition is called *homogeneous* if the probability of transition to the second state $|k\rangle$ is the same for all molecules or atoms in state $|i\rangle$. In this case the probability for the emission of electromagnetic radiation is given by:

$$P(\omega) = A_{ki}g(\omega - \omega_0) \quad (19)$$

Here, A_{ik} is the Einstein coefficient of spontaneous emission, $g(\omega - \omega_0)$ the previously introduced normalized Lorentzian profile.

2.4 Optical pumping

Now, a two-level system is considered, where electrons are excited to the higher energy level from the energetically lower level via *optical pumping*. Both levels shall be able to interact with each other by relaxation processes, but not with other levels. If we now introduce the probability P of a transition $1 \rightarrow 2$ by absorption, or $2 \rightarrow 1$ by emission and the relaxation probabilities of the respective levels with R_i , we find in *stationary* (i.e. $\frac{dN_i}{dt} = 0$) case the balance equation:

$$N_1 P + R_1 N_1 = N_2 P + R_2 N_2 \quad (20)$$

Implying conservation of the particle number $N = N_1 + N_2$ one can thus establish a relationship between N_i and the total particle number N :

$$N_1 = \frac{P + R_2}{2P + R_1 + R_2}; N_2 = \frac{P + R_1}{2P + R_1 + R_2} \quad (21)$$

In the absence of any pumping process $P = 0$, the expressions simplify to:

$$N_{10} = \frac{R_2}{R_1 + R_2}; N_{20} = \frac{R_1}{R_1 + R_2} \quad (22)$$

Also, it's interesting to note that in the case of $P \gg R_i$, both levels are exactly half occupied. Using N_{10} and N_{20} now ΔN can be expressed by ΔN_0 :

$$\Delta N = N_1 - N_2 = \frac{R_2 - R_1}{2P + R_1 + R_2} N = \frac{R_1 + R_2}{2P + R_1 + R_2} \Delta N_0 = \frac{1}{1 + \frac{2P}{R_1 + R_2}} \quad (23)$$

$$= \frac{1}{1 + S} \quad (24)$$

Here, the saturation parameter $S = \frac{P}{R}$ was introduced as $\bar{R} = \frac{R_1 + R_2}{2}$. Since also the absorption coefficient α is proportional to ΔN , it can be written as:

$$\alpha = \frac{\alpha_0}{1 + S} \quad (25)$$

A discussion for two levels, which also interact with other levels, can be found in [1].

2.5 Saturation broadening of homogeneously broadened transitions

In this section the shape of the frequency-dependent saturation parameter and the resulting line shape of the absorption coefficient in the case of saturation shall be discussed. Since, in the case of a monochromatic pump wave and a homogeneously broadened transition, the pump rate $P(\omega)$ has a Lorentzian profile, also $S(\omega) = \frac{P}{R}$ follows a Lorentzian profile:

$$S(\omega) = S_0 \frac{\left(\frac{\gamma}{2}\right)^2}{(\omega - \omega_0)^2 + \left(\frac{\gamma}{2}\right)^2}; S_0 = S(\omega_0) \quad (26)$$

To deduce from this the form of the frequency-dependent absorption coefficient, we consider the power absorbed for the transition from the energetically lower to the higher level:

$$\frac{d}{dt} W_{12}(\omega) = \hbar\omega P \Delta N = \hbar\omega \Delta N_0 \frac{S(\omega)}{1 + S(\omega)} \bar{R} \quad (27)$$

With (26) it can be modified to:

$$\frac{d}{dt} W_{ik}(\omega) = \hbar\omega \Delta N_0 \bar{R} \frac{S_0 \frac{\left(\frac{\gamma}{2}\right)^2}{(\omega - \omega_0)^2 + \left(\frac{\gamma}{2}\right)^2}}{1 + S_0 \frac{\left(\frac{\gamma}{2}\right)^2}{(\omega - \omega_0)^2 + \left(\frac{\gamma}{2}\right)^2}} = \hbar\omega \Delta N_0 \bar{R} \frac{S_0 \left(\frac{\gamma}{2}\right)^2}{(\omega - \omega_0)^2 + \left(\frac{\gamma}{2}\right)^2 (1 + S_0)} \quad (28)$$

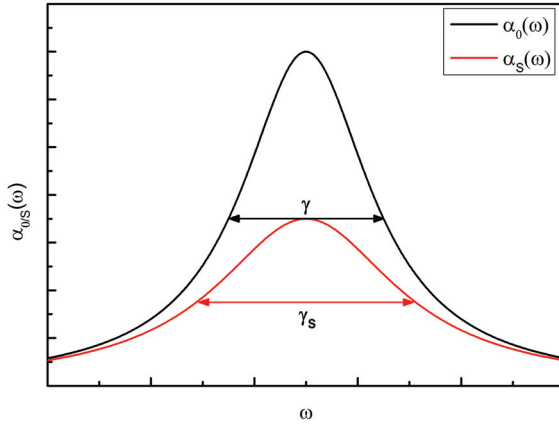


Figure 5: The Lorentzian profiles of the absorption coefficient without and with saturation.

The expression $(\frac{\gamma}{2})^2 (1 + S_0)$ is often called γ_S^2 . Since the absorption coefficient is proportional to the absorbed power of the transition, in the case of saturation it can also be represented by a Lorentzian profile with the line width γ_S :

$$\alpha_S(\omega) = \alpha_0(\omega_0) \frac{(\frac{\gamma}{2})^2}{(\omega - \omega_0)^2 + (\frac{\gamma_S}{2})^2} \quad (29)$$

From this general expression, the shape of the transition line should now be derived. At the center frequency ω_0 there is a reduction of the absorption coefficient by the factor

$$\frac{\alpha_S(\omega_0)}{\alpha_0(\omega_0)} = \frac{(\frac{\gamma}{2})^2}{(\frac{\gamma_S}{2})^2} = \left(\frac{\gamma}{\gamma_S}\right)^2. \quad (30)$$

For a frequency ω with a distance $|\omega - \omega_0| = \Delta\omega$ from the center frequency, the absorption coefficient is reduced by the factor

$$\frac{[\alpha_S(\omega)]}{[\alpha_0(\omega)]} = \frac{\left[\alpha_0(\omega_0) \frac{(\frac{\gamma}{2})^2}{(\Delta\omega)^2 + (\frac{\gamma_S}{2})^2} \right]}{\left[\alpha_0(\omega_0) \frac{(\frac{\gamma}{2})^2}{(\Delta\omega)^2 + (\frac{\gamma}{2})^2} \right]} = \frac{(\Delta\omega)^2 + (\frac{\gamma}{2})^2}{(\Delta\omega)^2 + (\frac{\gamma_S}{2})^2}. \quad (31)$$

Now it can be seen that the profile of the absorption coefficient is compressed in the case of saturation of a homogeneous transition with respect to the profile without saturation. Both functions are shown in figure 5. For saturation spectroscopy, it will be important to understand the saturation of heterogeneously broadened transitions, for example in the case of Doppler broadening. This is covered in section 2.7.

2.6 Linear and nonlinear absorption

To understand the broadening of non-homogeneously broadened transitions, first some background is set to the occurrence of *linear and nonlinear absorption*. Let us consider a monochromatic light wave $E = E_0 \cos(\omega t - k_x x)$ that propagates in x -direction, with the intensity $I = \frac{c\epsilon_0}{2} E_0^2$ and E_0 as the amplitude of the electric field. The absorbed power in volume $A dx$ is dx :

$$dP = AI\sigma_{ik} \left[N_i - \left(\frac{g_i}{g_k} \right) N_k \right] dx \quad (32)$$

The expression σ_{ik} denotes the absorption cross section of the molecules for the transition $|i\rangle \rightarrow |k\rangle$. In the case of a homogeneous line broadening and broadband irradiation with the spectral energy density $\rho = \frac{I(\omega)}{c}$, with $I(\omega)$ as spectral intensity density, one finds for the change in the population density of the absorbing level:

$$\frac{dN_i}{dt} = B_{ik} \frac{I(\omega)}{c} \left[\left(\frac{g_i}{g_k} \right) N_k - N_i \right] - N_i \gamma_i + \tilde{A}_i \quad (33)$$

In this expression, B_{ik} is the Einstein coefficient of absorption that differs from that of stimulated emission only by the factor $\left(\frac{g_i}{g_k} \right)$; $N_i \gamma_i$ denotes the total emptying rate through processes such as collisions, diffusion of molecules out of the excitation volume, or fluorescence; \tilde{A}_i denotes the total filling rate of the level, e.g. by diffusion of molecules into the excitation volume or fluorescence from higher energy levels. In the stationary case $\frac{dN_i}{dt} = 0$, filling and emission processes from the energetically higher level and emptying as well as absorption keep the balance. The stationary population density then results to:

$$N_i = \frac{\tilde{A}_i}{B_{ik} \frac{I(\omega)}{c} + \gamma_i} + N_k \frac{\left(\frac{g_i}{g_k} \right) B_{ik} \frac{I(\omega)}{c}}{B_{ik} \frac{I(\omega)}{c} + \gamma_i} \quad (34)$$

Now different limiting cases are looked at. First, we consider the low light intensity case *I*. Here, the absorption or stimulated emission rate becomes much smaller than the total emptying rate, so one can assume $B_{ik} \frac{I}{c} \ll \gamma_i$. In the limiting case of $I \rightarrow 0$, we obtain the so-called *thermal population density*, which is a very good approximation for most incoherent light sources (such as thermal light sources):

$$N_i^0 = \frac{\tilde{A}_i}{\gamma_i} \quad (35)$$

This corresponds to the ratio of filling to emptying rate.

On the other hand, if coherent light sources are considered (such as lasers), the intensity is usually large. Let us assume $B_{ik} \frac{I}{c} < \gamma_i$ is still valid, but $B_{ik} \frac{I}{c}$ is not negligibly small anymore, although the occupation of the level N_k is much smaller than that of the

level N_i . In this case, the second term in (34) can be neglected and one can develop the denominators first term into a Taylor series, by taking only its first term into account:

$$N_i = N_i^0 \frac{1}{1 + \frac{B_{ik}}{c\gamma_i} I(\omega)} \simeq N_i^0 \left(1 - \frac{B_{ik}}{c\gamma_i} I(\omega)\right) \quad (36)$$

Substituting this identity for N_i into (32), we see that the absorbed power for medium intensities under the above assumptions exhibits both a linear and a quadratic from I dependent term, respectively:

$$dP \simeq A\sigma_{ik} N_i^0 (I - \frac{B_{ik}}{c\gamma_i} I^2) dz \quad (37)$$

The quadratic part in this expression is called *saturation of the transition* $|i\rangle \rightarrow |k\rangle$ by optical pumping. By considering the limiting case of large intensities I , it follows $\frac{B_{ik}I}{c} \gg \gamma_i$ and the occupancy density of the absorbing level N_i results to:

$$N_i \simeq \frac{\tilde{A}_i}{\frac{B_{ik}I}{c}} + N_k \left(\frac{g_i}{g_k} \right) \quad (38)$$

It can be seen from this expression that for very large intensities the population densities of the two levels are equal. If we further consider the general expression for the frequency-dependent absorption, $\alpha(\omega) = [N_i - (\frac{g_i}{g_k}) N_k] \sigma_{ik}(\omega)$, we find that the absorption for $I \rightarrow \infty$ goes to zero. In other words the sample becomes transparent, which makes the use of the term *saturation* plausible.

In order to quantify the saturation of the individual levels, the saturation parameter $S_i = \frac{B_{ik}I}{c\gamma_i}$ is introduced. Now, (36) can be written as:

$$N_i = \frac{N_i^0}{1 + S_i} \quad (39)$$

The saturation of the gas depends in particular on the saturation of the transition $|i\rangle \rightarrow |k\rangle$, which can be characterized by the saturation coefficient of the transition, S_{ik} :

$$S_{ik} = \frac{2B_{ik}I}{c} \left[\frac{1}{\gamma_i} + \frac{1}{\gamma_k} \right] \quad (40)$$

The *saturation intensity* is now further defined as the intensity at which $S_{ik} = 1$, i.e. as:

$$I_s = \frac{c}{2B_{ik}} \frac{\gamma_i \gamma_k}{\gamma_i + \gamma_k} \quad (41)$$

After some calculations, for the population densities in the case of saturation with homogeneous line broadening one obtains for $S \ll 1$:

$$N_i(\omega) = N_i^0 - \frac{\Delta N^0}{\gamma_i \tau} \frac{S_0 \left(\frac{\gamma}{2} \right)^2}{(\omega - \omega_0)^2 + \left(\frac{\gamma_S}{2} \right)^2} \quad (42)$$

$$N_k(\omega) = N_k^0 + \frac{\Delta N^0}{\gamma_k \tau} \frac{S_0 \left(\frac{\gamma}{2} \right)^2}{(\omega - \omega_0)^2 + \left(\frac{\gamma_S}{2} \right)^2} \quad (43)$$

with $\tau = \frac{\gamma}{\gamma_i \gamma_k}$ and $\gamma = \gamma_i + \gamma_k$.

2.7 Saturation broadening of inhomogeneously broadened transitions

If one now assumes a certain temperature in the gas under study, as described above the individual atoms obey a Maxwell-Boltzmann distribution and the frequencies in the population densities in equation (42) and equation (43) shift according to the velocities of the individual atoms or molecules:

$$N_i(\omega, v_x) = N_i^0 - \frac{\Delta N^0}{\gamma_i \tau} \frac{S_0 \left(\frac{\gamma}{2}\right)^2}{(\omega - \omega_0 - kv_x)^2 + \left(\frac{\gamma_S}{2}\right)^2} \quad (44)$$

$$N_k(\omega, v_x) = N_k^0 + \frac{\Delta N^0}{\gamma_k \tau} \frac{S_0 \left(\frac{\gamma}{2}\right)^2}{(\omega - \omega_0 - kv_x)^2 + \left(\frac{\gamma_S}{2}\right)^2} \quad (45)$$

The difference in the population densities of the two individual levels $\Delta N(\omega, v_x) = N_i(\omega, v_x) - N_k(\omega, v_x)$ results to:

$$\Delta N(\omega, v_x) = \Delta N^0(v_x) \left(1 - \frac{S_0 \left(\frac{\gamma}{2}\right)^2}{(\omega - \omega_0 - kv_x)^2 + \left(\frac{\gamma_S}{2}\right)^2} \right) \quad (46)$$

In this distribution a hole is created called *Bennet hole*. In preparation for the experiment, it is a good exercise to calculate the depth and the homogeneous width of this hole analogously to the previous procedure. Since one can not measure the population densities directly, one is interested in the spectral intensity distribution of a laser beam after passing through the gas cell. An intermediate quantity the frequency-dependent absorption coefficient is calculated to which the measured intensity is proportional. It results to:

$$\alpha(\omega) = \int \Delta N(v_x) \sigma(\omega, v_x) dv_x \quad (47)$$

Interestingly, using the specific expressions for each factor one obtains again a Voigt function:

$$\alpha(\omega) = \frac{\Delta N^0 \sigma_0}{v_p \pi} \int \frac{\exp \left(\frac{v_x}{v_p} \right)^2}{(\omega - \omega_0 - kv_x)^2 + \left(\frac{\gamma_S}{2} \right)^2} \quad (48)$$

In good approximation calculation of this integral is possible even analytically. The procedure is explained in [1]. In particular, it can be seen that the holes in the population density do not lead to holes in the spectral distribution of the absorption coefficient. Therefore, one can not measure them with the standard setup used here! Instead, it is found that when using anti-collinear pumping and probe laser beams, with the latter having a much lower intensity, an absorption profile of the following form is found (detailed derivation in [1] and references therein):

$$\alpha_S(\omega) = \alpha^0(\omega) \left(1 - \frac{S_0}{\sqrt{1+S_0}} \frac{\left(\frac{\gamma}{2}\right)^2}{(\omega - \omega_0 - kv_x)^2 + \left(\frac{\gamma[1+(1+S_0)^{\frac{1}{2}}]}{2}\right)^2} \right) \quad (49)$$

Since $\alpha^0(\omega)$ has a Gaussian profile, $\alpha_S(\omega)$ is also a Gaussian profile but with a hole in the middle of the line, which is called *Lamb dip*. This means that exactly at the resonant frequencies ω_0 the two waves are absorbed by molecules of the same "velocity category" (namely without a component in the x -direction). In the above calculations it was assumed that $S_0 \ll 1$ and that the wavelengths of pump and probe laser differ only insignificantly. As shown in chapter 6, this condition is fulfilled in our case, since we branch off the probe beam via a beam splitter and subsequent attenuation from the pumping beam, i.e. they exhibit the same frequency and wavelength.

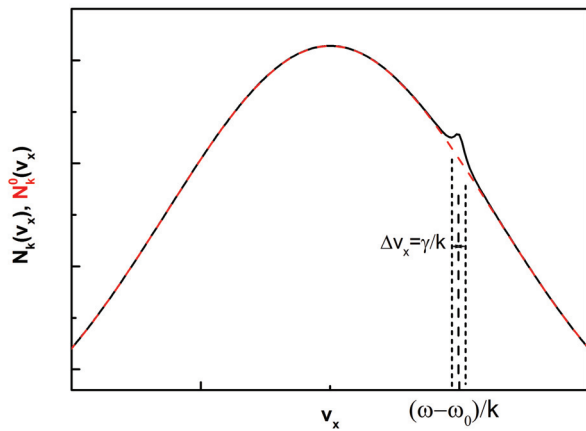
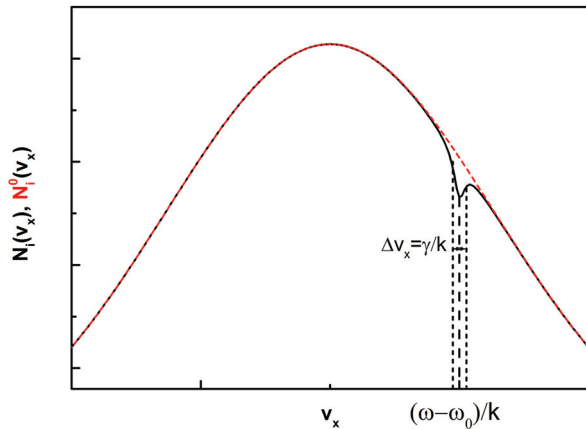


Figure 6: Decrease or increase the population densities of heterogeneously broadened transitions at saturation.

3 Origin of fine structure and hyperfine structure

3.1 Fine structure

Due to coupling of the orbital angular momentum \vec{L} and the spin \vec{S} of the electron, a contribution of this interaction in the Hamiltonian arises, which is proportional to the product of \vec{L} and \vec{S} :

$$H = H_0 + H_{FS} \quad (50)$$

$$H_{FS} \propto \vec{L} \cdot \vec{S} \quad (51)$$

Since \vec{L} and \vec{S} no longer commute with the overall Hamiltonian H , l and s are no longer quantum numbers. However, since $\vec{J} = \vec{L} + \vec{S}$ commutes with the Hamiltonian, j and j_z are suitable quantum numbers. They correspond to the projection of \vec{J} onto the z component of \vec{J} . The problem can be tackled with perturbation theory of first order, since the contribution of the interaction term is two orders of magnitude smaller than the contribution of the interaction-free Hamiltonian H_0 . j takes values of $|l - s| \leq j \leq l + s$. Rubidium has the electron configuration $[Kr]5s^1$. So, in the ground state it is $s = \frac{1}{2}$ and $l = 0$, for $j = \frac{1}{2}$. In spectroscopic terminology this state is called $5^2S_{\frac{1}{2}}$. For the first excited state one finds $l = 1$, $s = \frac{1}{2}$ and thus $j = \frac{1}{2}, \frac{3}{2}$. These two components are called $5^2P_{\frac{1}{2}}$ and $5^2P_{\frac{3}{2}}$.

Transitions can occur between the ground state and the two excited states, as evidenced in the spectrum. The resulting lines are called the D_1 and D_2 lines:

$$D_1 : 5^2S_{\frac{1}{2}} \rightarrow 5^2P_{\frac{1}{2}} \quad (52)$$

$$D_2 : 5^2S_{\frac{1}{2}} \rightarrow 5^2P_{\frac{3}{2}} \quad (53)$$

The resonance frequencies of these two lines are $\nu_{D_1} = 377.1\text{THz}$ and $\nu_{D_2} = 384.2\text{THz}$. In this experiment only the D_2 -line of rubidium will be experimentally investigated.

3.2 Hyperfine structure

In addition to the electron, also the nucleus has an intrinsic angular momentum, the nuclear spin \vec{I} . It interacts with the total angular momentum \vec{J} and causes another, albeit small, splitting of the lines. Similar to fine structure, the interaction between nuclear spin and the total angular momentum of the electron is proportional to $\vec{J} \cdot \vec{I}$. By adding this term, \vec{J} no longer commutes with the overall Hamiltonian. Instead, analogous to the fine structure, the sum of the angular momentum $\vec{F} = \vec{J} + \vec{I}$ commutes with $H_{ges,HFS}$. The eigenvalues of \vec{F} are given by $|j - i| \leq f \leq j + i$. The element rubidium is present in nature (and thus also in the gas cell!) with a natural isotopic mixture of 72.2% ^{85}Rb and 27.8% ^{87}Rb . Since the number of neutrons differs in both isotopes, they exhibit a different nuclear spin. For ^{85}Rb , the eigenvalue of the nuclear

spin is $i = \frac{3}{2}$, while for ^{87}Rb is the nuclear spin $i = \frac{5}{2}$. Hence, for the ground and excited states, the following values are obtained for f :

ground state :

$$^{85}\text{Rb} : j = \frac{1}{2}, i = \frac{3}{2} \rightarrow f = 1, 2 \quad (54)$$

$$^{87}\text{Rb} : j = \frac{1}{2}, i = \frac{5}{2} \rightarrow f = 2, 3 \quad (55)$$

excited state :

$$^{85}\text{Rb} : j = \frac{1}{2}, i = \frac{3}{2} \rightarrow f = 1, 2 \quad (56)$$

$$^{85}\text{Rb} : j = \frac{3}{2}, i = \frac{3}{2} \rightarrow f = 0, 3 \quad (57)$$

$$^{87}\text{Rb} : j = \frac{1}{2}, i = \frac{5}{2} \rightarrow f = 2, 3 \quad (58)$$

$$^{87}\text{Rb} : j = \frac{3}{2}, i = \frac{5}{2} \rightarrow f = 1, 4 \quad (59)$$

The energetic splittings are shown quantitatively and as schemes in [3] and [4].

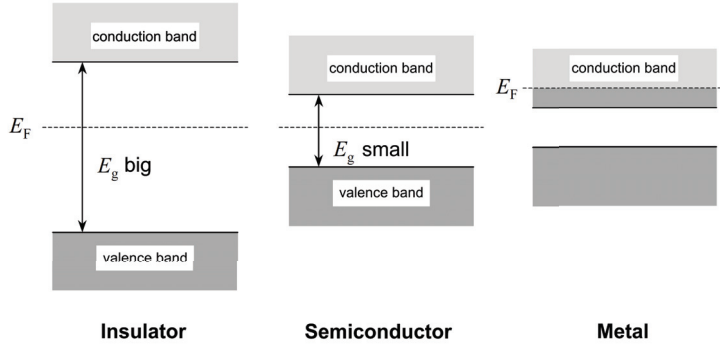


Figure 7: Location of the Fermi level in metals, semiconductors and insulators. Taken from [5].

4 Structure of a laser diode

For this experiment, a coherent light source is needed that is inexpensive to manufacture and can be tuned to specific wavelengths by changing temperature and current. These properties are comprised by a laser diode, a semiconductor-based device.

This component is based on a so-called p-n junction, which is supplemented by further elements depending on the application. In this section the basics of these technologies are explained.

4.1 Introduction to semiconductors

Semiconductors are materials (usually solids) with an electrical conductivity between those of the metals and those of the insulators. For metals under standard conditions, there is a large number of free electrons that can be described as electron gas. Insulators are non-conductive under standard conditions. The reason for these phenomenological differences is the differing energetic structure of these materials. The periodic arrangement of the atoms in a solid and the concomitant densification of the atomic energy levels leads to the formation of various quasi-continuous energy bands, which are separated by a band gap. All bands above the band gap are called conduction bands and all below the band gap valence bands. Often, simply the lowest conduction band is called conduction band, and the valence band with the highest energy is called valence band.

In metals, the highest occupied energy level is in the conduction band and coincides with the so-called Fermi level. The electrons above the conduction band edge, i.e. above the energetically lowest edge of the conduction band, can move freely through the metal in the context of the approximation for an electron gas. In the case of an intrinsic (i.e. undoped; see below) semiconductor, the Fermi level lies in the middle of the band gap – at the Fermi level, there are no allowed energy levels. The different situations are shown in figure 7. In semiconductors, electrons can be transferred from the valence band into the conduction band by thermal or optical excitation, where they can contribute to the

conductivity of the material. In particular, the conductivity of a semiconductor increases for rising temperatures.

Semiconducting substances are, for example, elements of the fourth main group, such as silicon or germanium, and compounds of elements of the third and fifth main groups, so-called III-IV compounds, such as *GaA*, *GaP*, *GaN*, *InAs* or *InSb*. To tailor materials with specific band gaps, mixed crystals such as *GaAs_{1-x}P_x*, *GaAlAsSb* or *GaInAsP* are assembled. In such materials the band gap is derived from empirical formulas that account for the ratio of the individual compounds inside the mixed crystal .

Semiconductors become useable and useful because of the option of doping. Doping is the replacement of some atoms in the crystal lattice by other atoms. If these impurities have a higher coordination valence than the replaced atom it is called *n*-doping, e.g. for phosphorus in silicon. This name refers to the ability of the phosphorus atom to emit an electron to the lattice (because of its higher number of electrons), which can move nearly freely through the lattice. In the case of doping with atoms of lower coordination valence it is called *p*-doping, e.g. for boron in silicon. Here, the missing electron creates a positively charged "hole" compared to the lattice, which can move in the same way as the electron in the lattice. In the energy scheme one can look more closely at the processes: By introducing a "foreign atom", a level within the band gap is created, e.g. in the case of *n*-doping, a level near the conduction band edge. It can be calculated that the Fermi level lies in this case quite exactly in the middle between the doped level and the conduction band edge. Because the energy gap between the donor level and the conduction band edge is rather small, a thermal excitation (at room temperature in the range of about 5 meV) is sufficient to lift the electron from the donor level into the conduction band where it contributes to the conductivity. In the case of *p*-doping, i.e. in the case of introducing acceptors, the conditions are analogous. Here, the energy between acceptor level and valence band edge is reduced and a hole is excited into the valence band by the thermal energy. Depending on whether in a semiconductor the conductivity is due to electrons or holes, they are classified as *n*- or *p*-semiconductor.

It should be noted that both, the electrons and the holes in the semiconductor are so-called quasi-particles, in contrast to free electrons (which are particles). This means that they are assigned a so-called effective mass, which includes the influences of the crystal lattice and the other charge carriers. Therefore, within this model, an electron or hole moves like a free electron of mass m_{eff} in the crystal. The effective mass of the holes is usually larger than the effective mass of the electrons.

The corresponding charge carrier densities of the electrons and the holes are given by:

$$n = \int_0^{\infty} g_c(\epsilon) f_e(\epsilon) d\epsilon \quad (60)$$

$$p = \int_0^{\infty} g_c(\epsilon) f_h(\epsilon) d\epsilon \quad (61)$$

Here, n and p are the carrier densities of the electrons or holes, respectively; $g_c(\epsilon)$ the energetic state densities and $f_{e/h}$ the Fermi distribution functions for the electrons and holes, respectively. The relation $f_h(\epsilon) = 1 - f_e(\epsilon)$ applies. ϵ are the energies $\epsilon = E - E_c$ counted from the conduction band edge. Strictly speaking, these equations are approximations, assuming that the energy in the entire spectrum depends quadratically on the wave vectors \vec{k} . This is not correct, as this approximation applies only to small values of k . However, it is a good approximation owing to the fact that the product of state density $g_c(\epsilon)$ and Fermi distribution functions $f_{e/h}$ is included in the equations with the latter rapidly vanishes with increasing ϵ . Assuming that the considered energies of the occupied states lie far away from the band edge (as explained above, this is a reasonable approximation in most cases), the Fermi distribution can be approximated by

$$f_e(E) = \frac{1}{1 + \exp\left(\frac{E - E_F}{k_B T}\right)} \approx \exp\left(-\frac{E - E_F}{k_B T}\right) \quad (62)$$

and one obtains for n and p after some calculations (see e.g. [5] or [6])

$$n = N_C \exp\left(\frac{E_F - E_C}{k_B T}\right) \quad (63)$$

$$p = N_V \exp\left(\frac{E_V - E_F}{k_B T}\right) \quad (64)$$

N_C and N_V are referred to as *effective state densities* of the conduction and valence band edges, respectively. Since the Fermi level is usually not known at first, it would be desirable to find an expression in which the carrier concentrations only depends on material parameters N_C , N_V and on the band gap energy E_g . It can be obtained by using the *law of mass action* from chemistry and by applying it to the "reaction"



One thus finds

$$np = N_C N_V \exp\left(-\frac{E_C - E_V}{k_B T}\right) = N_C N_V \exp\left(-\frac{E_g}{k_B T}\right) \quad (66)$$

In an intrinsic semiconductor, holes and electrons are always generated in pairs. Therefore, the number of holes is equal to the number of electrons and thus we obtain the so-called *intrinsic carrier concentration* n_i :

$$n_i = \sqrt{np} = \sqrt{N_C N_V} \exp\left(-\frac{E_g}{2k_B T}\right) \quad (67)$$

4.2 Doping of semiconductors

Now question shall be addressed how to change the charge carrier concentrations in the presence of impurities. First, we assume the material to be n -doped, i.e. all introduced

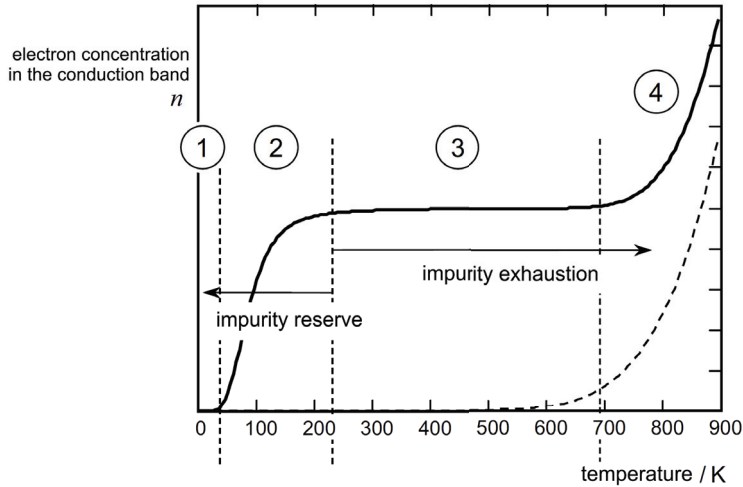


Figure 8: The conductivity of a n -doped semiconductor as a function of the temperature. The described regimes are clearly visible. The picture was taken from [5].

impurities are donors. The density of impurities in the material is given by N_D . Now you have to distinguish different temperature regimes in which the impurities are ionized differently.

At very low temperatures, the thermal energy is insufficient to excite the electrons from the donor levels into the conduction band. Since electrons from the valence band require an even larger excitation energy to move into the conduction band, no electrons are excited into the conduction band in this way either. Thus, there are no free charge carriers and the carrier density is $n = 0$.

At slightly higher temperatures, some of the electrons are already ionized from the impurity levels, but excitation from the valence band still does not occur. The number of electrons is thus equal to the number of ionized impurities, i.e. $n = N_D^+$. This is called *impurity reserve*.

Interesting for application is the case of so-called *impurity exhaustion*, which usually occurs at room temperature. Here, the impurity levels are fully ionized, while the number of electrons changing from the valence band into the conduction band (and, in turn, holes that change from the conduction band to the valence band) can still be neglected. One thus obtains $n = N_D$.

At very high temperatures, the electrons excited from the valence band into the conduction band also contribute to the charge carrier density, so that the charge carrier density after a transition zone corresponds to the intrinsic carrier density $n = n_i$. The different regimes are shown in the figure 8. For a quantitative analysis again [6] and [5] are recommended.

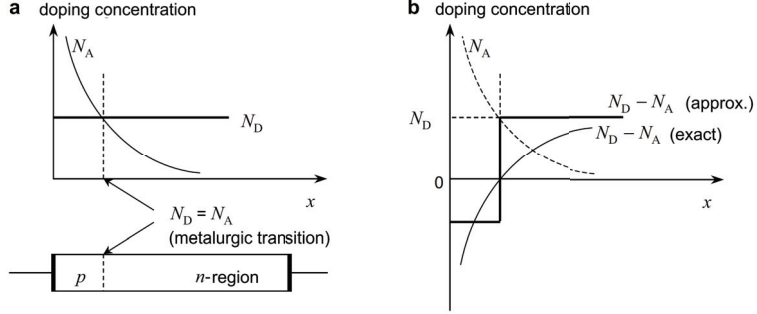


Figure 9: The real (a) and approximated (b) doping profiles at the p-n junction. The picture was taken from [5].

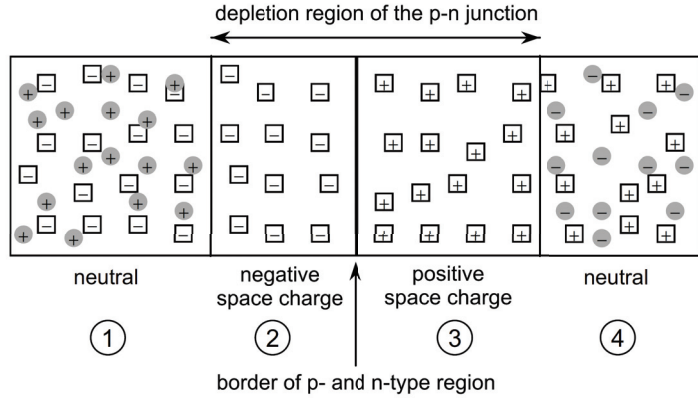


Figure 10: The model for the free charge carriers and the stationary charge hulls at the p-n junction. The picture was taken from [5].

4.3 p-n junction without external voltage

The p-n junction is the simplest form of a semiconductor device. It is a layered sequence of a *n*- and a *p*-doped semiconductor. The fabrication of such a structure is usually done by diffusing acceptors into *n*-doped material and overcompensating the *n*-doping. Generally, a step-shaped doping profile is used to describe the transition, with $N_D = 0$ on the one side (left in figure 9) and $N_A = 0$ on the other (right side in the figure) applies. Thus one obtains the doping model shown in figure 10. In the *p*-region, holes are the mobile charge carriers, while in the *n*-region the charge carriers are the electrons. At the boundary between the two areas, recombination of charge carriers takes place by diffusion processes, so that after setting an equilibrium no free charge carriers are present there. Instead, negative (*p*-area) or positive (*n*-area) stationary charge hulls are formed. This area is called *space-charge region*.

By these stationary charges an electric field is formed, which can be described by the

Poisson equation:

$$\rho(\vec{r}) = -\epsilon\epsilon_0 \nabla \cdot \nabla U(\vec{r}) \quad (68)$$

In the one-dimensional case with change of the charge carrier concentration in x -direction, the Poisson equation reduces to:

$$\rho(x) = \epsilon\epsilon_0 \frac{d\mathcal{E}(x)}{dx} \quad (69)$$

Charge carrier density, electric field and voltage across the p-n junction are shown in figure 11. The derivation of numerous parameters such as the width of the space-charge regions or the potential curve can be found in [5].

In fact, the model described above is quite simple and does not accurately reflect reality. In particular, free charge carriers also diffuse into the space-charge zone, resulting in a logarithmic drop of the charge carriers across the space-charge region. Assuming that the *drift current* induced by the electric field and the diffusive fluxes generated by the concentration gradients balance each other for both types of charge, one obtains after some calculation (see e.g. [5]) for the *Diffusion potential*, i.e. the voltage difference between the two ends of the space-charge region, the expression:

$$U_D = \frac{k_B T}{e} \ln \frac{N_D N_A}{n_i^2} \quad (70)$$

4.4 p-n junction with external voltage

By applying an external voltage to the p-n junction with the positive pole connected to the p -doped region and the negative pole to the n -doped region, the holes are "sucked" into the n -doped region and the electrons into the direction of the p -doped area. Thus, the space-charge zone decreases and the voltage across the junction just decreases by the amount of the applied voltage. This polarity is denoted with *conducting* or *forward direction*.

The reversed polarity of the junction is called *reverse direction*. Here, the space-charge region increases and the barrier height increases by the amount of the applied voltage.

4.5 Laser diode

4.5.1 Basics and laser conditions

So far, it has only been considered that charge carriers can change from the valence band or impurity levels into the conduction band. However, also an optical excitation is possible. By *absorption* of a photon whose wavelength corresponds to (or slightly exceeds) an energetic transition, electron-hole pairs are generated in conduction and valence bands, which may contribute to the conductivity in the semiconductor. On the other hand, by recombination of a hole in the valence band with an electron in the conduction band,

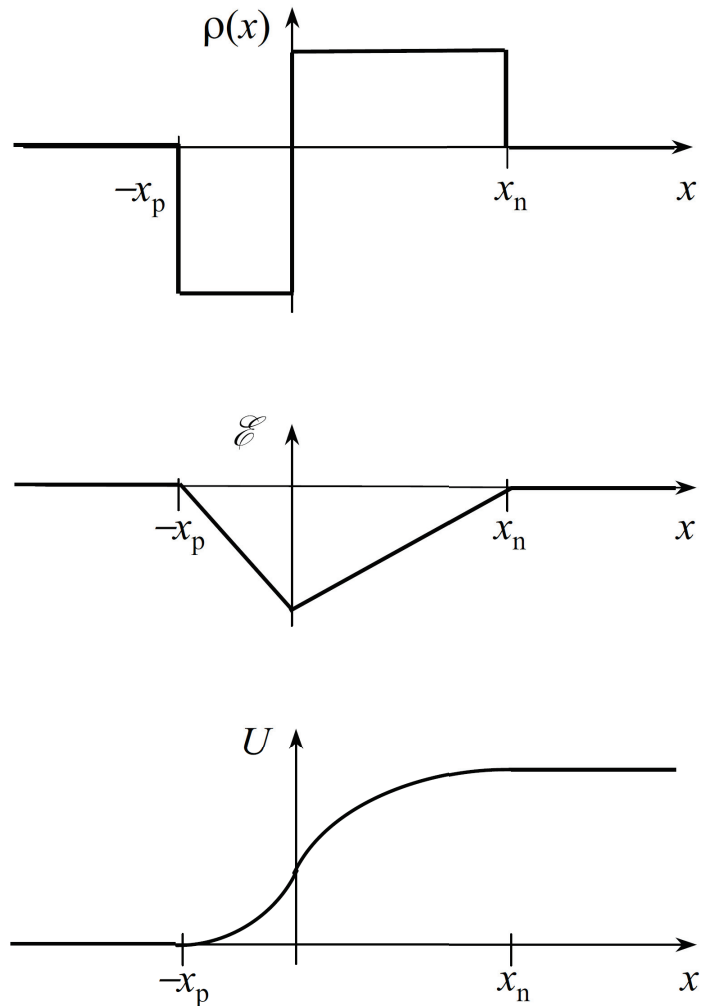


Figure 11: Charge carrier density, field and voltage across the p-n junction. The picture was taken from [5].

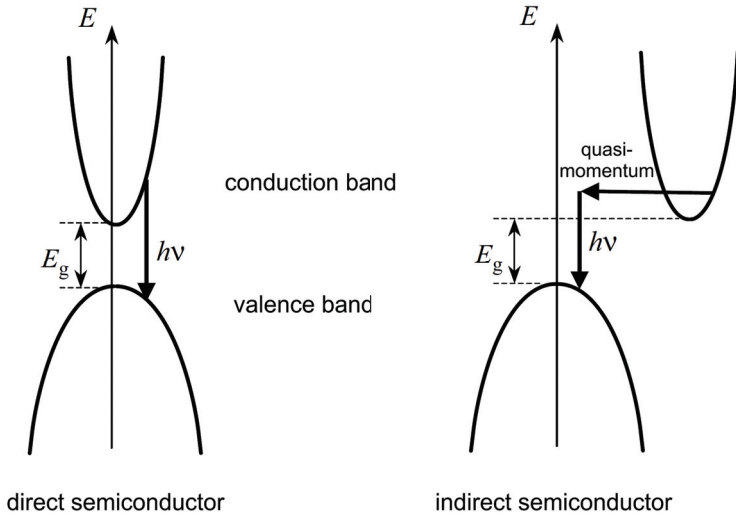


Figure 12: Emissions in direct and indirect semiconductors. The picture was taken from [5].

a photon is released with an energy corresponding to the energetic distance of the two quasi-particles in the band diagram. This process is called *spontaneous emission*. Since a photon has only a very small momentum, absorption and spontaneous emission occur together with a hole-electron pair and a photon only vertical in the E - k diagram.

Before considering the construction and important parameters of a laser diode, we need to clarify the difference between so-called *direct* and (*indirect*) semiconductors. Looking at the band structure of a semiconductor, one can fundamentally distinguish the two cases in which the conduction band minimum and the valence band maximum are at the same k value (direct) or at different k values (indirect). Since k corresponds to a crystal quasi-impulse via $p_q = \hbar k$, reaching levels at another k value is only possible with generation of *phonons*, i.e. quantized lattice vibrations. Thus, in contrast to a maximum-minimum transition in a direct semiconductor, this involves a three (quasi-)particle process. Upon emission, an electron and a hole recombine and a phonon of the appropriate wavelength is released. Conversely, at the same time a phonon of the appropriate wavelength would have to be absorbed during absorption. As such processes are highly improbable, typically only direct semiconductors such as *GaAs* or *GaN* are suitable for opto-electronic applications. An exception is *GaP*, in which nitrogen atoms can be incorporated at the position of phosphorus as *isoelectric impurities*. Due to their smaller size, the material exhibits a greater uncertainty in the momentum space according to the Heisenberg uncertainty principle and transitions with $\Delta p_q \neq 0$ become more probable. The emission behavior in direct and indirect semiconductors is shown schematically in figure 12.

Now let us consider the construction of a laser diode. A laser is a light source that can emit very *coherent* and *monochromatic light*. Semiconductor lasers have low power com-

pared to other types of lasers, such as gas lasers or other solid state lasers like as ruby, but are well suited for high frequency modulation and fiber optic coupling. Materials for lasers are for example *GaAs*, *GaInAsP* or *GaAlAsSb*.

In contrast to other optoelectronic devices such as Light Emitting Diodes, where the light is generated incoherently by spontaneous emission, the operation of a laser requires *stimulated emission*. Stimulated emission is a process in which the presence of a radiation field excites the recombination of electron-hole pairs by photons of the appropriate wavelength. When such excitation occurs, the recombining electron-hole pair not only emits radiation of the same wavelength as the exciting photon, but also with the same phase and direction. In other words one gets a "copy" of the stimulating photon. Stimulated and spontaneous emission always happen simultaneously. For lasing to take place, the stimulated emission must outweigh the spontaneous emission. To achieve this situation the laser diode is built as *optical resonator*, i.e. as an area bounded by two highly reflective mirrors and whose length L is tailored to the emission wavelength of the material ($L = \frac{m\lambda}{2}$, with m as natural number). Ideally, L should be as large that the *laser mode* with $m = 1$ is already possible. In such a resonator, waves of the appropriate wavelength constructively interfere with each other so that amplification occurs. In fact, the *gain* (see below) is too small in such structures, which requires construction of longer resonator structures. Therefore, the wavelength difference between adjacent modes becomes progressively smaller and such a laser typically have multiple modes (instead of ideally only one).

On the other hand, we have already pointed out that absorption and emission processes are proceeding continuously in the semiconductor. If emitted photons are directly absorbed again, they are not available for stimulated emission. Therefore, the difference of spontaneous emission and absorption must be as large as possible. This difference is called *gain g* and is calculated as:

$$g = I_{sp} - I_{abs} = w_{eh}g_{eh}(h\nu) [f_e f_h - (1 - f_e)(1 - f_h)] = w_{eh}g_{eh}(h\nu) [f_e - (1 - f_h)] \quad (71)$$

In this equation w_{eh} stands for the (optical transition probability), which is in good approximation independent of the energy of the transition. $g_{eh}(h\nu)$ is the combined state density of the transition (total number of the transition states per energy interval of energetically stacked levels of electrons and holes). The condition of $g > 0$ means that the number of electrons in a certain state in the conduction band (in the energetically higher level) f_e should be larger than the number of electrons in the associated valence band state $(1 - f_h)$. This condition is called *population inversion*.

In summary, two conditions have to be met for lasing:

- A suitable optical amplifier (resonator) must be present, in which the electromagnetic waves can amplify themselves and form steady waves.
- A population inversion must be established to reach a *gain* above zero

4.5.2 Realizations

In laser diodes, it is important to keep the light in the device as long as possible so that it is available for stimulating (stimulated emission). Therefore, the laser diodes are realized as *edge emitters* with the edges of the active area polished to act as mirrors. Of course, radiation is permanently released as the reflection coefficient $R = \frac{(n-1)^2}{(n+1)^2}$ is quite small; in the case of GaAs ($E_g \approx 3.66$) it is $R \approx 0.33$. In order to keep the losses as low as possible often so-called *double heterostructure laser* (or *DH-Laser*) are realized, i.e. structures where the active region of the laser diode is surrounded by two regions with larger band gap. Since the band gap is in good approximation inversely proportional to the refractive index of the material, there is a "guiding" of the light or even total reflection occurs. The laser diode used in the experiment has an emission wavelength of 780.0 nm at standard conditions.

4.5.3 Tuning the laser diode

The emitted wavelength of the laser diode depends on three parameters:

- the temperature of the laser,
- The current injected into the laser diode,
- The position and orientation of the laser grid.

In the experimental setup the temperature of the laser as well as the injected current should be varied. As the temperature of the laser increases, the active zone expands and the wavelength of the laser is increased to $L = \frac{m\lambda}{2} = \frac{mc}{2\nu}$. Since the temperature is not immediately constant throughout the device, it is necessary to wait between two measurements at different temperatures for about 10 minutes. When increasing the injection current, the temperature increase takes place directly in the active zone and the resulting frequency reduction occurs faster. Since the laser never operates completely monomode-like, so-called mode jumps may occur if temperature and injection current are varied. This means, within a narrow temperature or frequency interval it switches from a main mode of the laser to an adjacent mode. One task of the experimental part is to record one or, ideally, several such transitions from one mode to the next by varying the injection current in small steps at a fixed temperature.

For more information about the influence of these parameters on the emission properties, see for example [7].

5 Set-up of a Fabry-Pérot interferometer (FPI)

A Fabry-Perot interferometer (FPI) consists of two parallel, highly reflecting surfaces in a certain distance to each other. Between the two surfaces an electromagnetic wave can be reflected back and forth. It is the simplest case of an optical resonator for electromagnetic waves of an appropriate frequency. For a quantitative description, the physical description of this process for a monochromatic wave will be considered below. The two highly reflective surfaces may have the distance d , the electromagnetic wave coupled into the resonator has the frequency ν and, correspondingly, the wavenumber $k = \frac{2\pi\nu}{c}$ where c is the speed of light. The wave itself can be described by

$$\phi(r, t) = U(r)\exp(i\omega t) \quad (72)$$

with $\omega = 2\pi\nu$. The amplitude of this wave shall satisfy the Helmholtz equation (see, e.g. [8]), i.e.:

$$\nabla^2 U(r) = -k^2 U(r) \quad (73)$$

from which it immediately follows that $U(r) = U_0 \text{Im}[\exp(ikr)]$. For a resonant wave inside the resonator, the boundary condition must be fulfilled that ϕ disappears on both edges, i.e. it must hold: $\phi(r = 0, t) = \phi(r = d, t = 0)$, which is true if and only if $k_n = \frac{\pi n}{d}$. These k_n are resonator modes that correspond to the resonant frequencies $\nu_n = \frac{c}{\lambda_n} = \frac{ck_n}{2\pi} = \frac{nc}{2d}$. The frequency spacing between two adjacent resonant modes thus results in $\frac{[(n+1)-n]c}{2d} = \frac{c}{2d}$. This frequency spacing is known as the Free Spectral Range (FSR).

Now we consider a wave that is reflected back and forth several times in a resonator of length d . The amplitude of the wave decreases with each reflection by the factor r , which is called reflectivity. Furthermore, there is a phase difference $\phi = k2d$ between the original wave and each reflected wave. The factor two is caused by the wave traversing d twice until it returns to its original location. Constructive interference occurs if the phase difference equals a multiple of 2π , hence at $\phi = n2\pi$. With $k = \frac{2\pi\nu}{c}$, one obtains from $\frac{4\pi\nu d}{c} = 2\pi n$ the same free spectral range as above: $\nu = \frac{nc}{2d} \rightarrow FSR = \frac{c}{2d}$. The total amplitude of the interfering waves results in:

$$U = U_0 + r \exp(i\phi)U_0 + (r \exp(i\phi))^2 U_0 + \dots \quad (74)$$

This corresponds to a geometric series:

$$\sum_{n=0}^{\infty} q^n = \frac{1}{1-q} \quad (75)$$

with $q = r \exp(i\phi)$, since the absolute value of this expression is smaller than 1 (the absolute value of $\exp(i\phi)$ is 1 and $r < 1$). As U_0 is a common factor it follows:

$$U = \frac{U_0}{1 - r \exp(i\phi)} \quad (76)$$

The physically measurable quantity is the intensity of the electromagnetic radiation. It results from the square of sums U :

$$I = |U|^2 = |U_0|^2 \frac{1}{1 - r \exp(i\phi)} \frac{1}{1 - r \exp(-i\phi)} \quad (77)$$

$$= |U_0|^2 \frac{1}{1 - r \exp(i\phi) - r \exp(-i\phi) + r^2} = |U_0|^2 \frac{1}{1 - 2r \cos(\phi) + r^2} \quad (78)$$

Using the following relationship makes this expression can be simplified:

$$\exp\left(\frac{i\phi}{2}\right) \exp\left(\frac{i\phi}{2}\right) = \exp(i\phi) \quad (79)$$

$$\Leftrightarrow \left(\cos^2\left(\frac{\phi}{2}\right) - \sin^2\left(\frac{\phi}{2}\right) \right) + i\dots = \cos(\phi) + i\dots \quad (80)$$

With the known relations for sine and cosine we obtain:

$$\cos(\phi) = 1 - 2 \sin^2\left(\frac{\phi}{2}\right) \quad (81)$$

Thus, the intensity can also be written as::

$$I = \frac{I_0}{(1 - r)^2 + 4r \sin^2\left(\frac{\phi}{2}\right)} = \frac{I_{max}}{1 + \left(\frac{2\mathcal{F}}{\pi}\right)^2 \sin^2\left(\frac{\phi}{2}\right)} \quad (82)$$

$\mathcal{F} = \frac{\pi\sqrt{r}}{1-r} = \frac{\pi}{T+L}$ is the finesse of the interferometer and $I_{max} = \frac{I_0}{(1-r)^2} = \frac{|U_0|^2}{(1-r)^2}$. With the help of this formula, we now calculate the full width at half maximum of the transmission peaks. Looking closer at (82), we see that the intensity just becomes maximum for $\phi = \frac{2\pi\nu}{\nu_F} = n$, as the contribution of the sine-terms disappears. Accordingly, one obtains the distance to the next frequency at which the intensity becomes half maximum by requesting:

$$1 + \left(\frac{2\mathcal{F}}{\pi}\right)^2 \sin^2\left(\frac{\pi\nu}{\nu_F}\right)^2 = 2 \quad (83)$$

$$\Leftrightarrow \left(\frac{\pi}{2\mathcal{F}}\right)^2 = \sin^2\left(\frac{\pi\nu}{\nu_F}\right) \quad (84)$$

$$\Leftrightarrow \left(\frac{\pi}{2\mathcal{F}}\right)^2 = \sin^2\left(\frac{\pi\nu}{\nu_F}\right) \quad (85)$$

For example, by assuming $r = 0,33$ we obtain $\frac{\pi}{2\mathcal{F}} \approx 0,58$ and with $\arcsin(0.58) \approx 0.62$ a rather similar value. Thus we can use the small-angle approximation for the sine function with $\sin(x) \approx x$. This yields the catchy expression for the FWHM $\delta\nu$ (twice the calculated expression):

$$\delta\nu = \frac{\nu_F}{\mathcal{F}} \quad (86)$$

The typical transmission spectrum of a Fabry-Pérot interferometer is shown in figure 13. In the present experimental setup the free spectral range is FSR = 1GHz. The

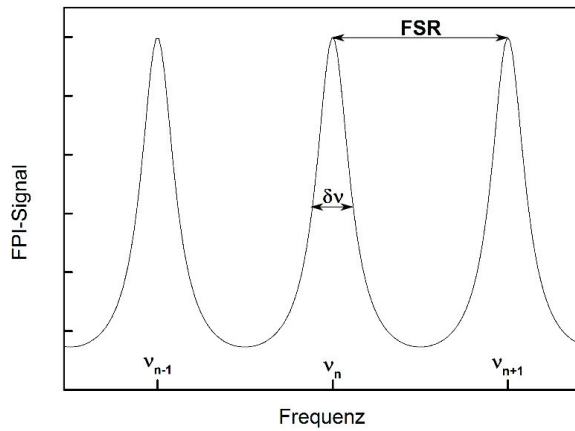


Figure 13: Close-up view of the transmission spectrum of a Fabry-Pérot interferometer. The free spectral range and the FWHM of the peaks are indicated.

Fabry-Pérot interferometer is not realized using planar mirrors but by confocal spherical mirrors. Further information and specifications can be found in the document "Fabry-Perot Interferometer Manual" at the lab desk.

An example for the use of a Fabry-Pérot interferometer for frequency control is demonstrated at the cesium D_2 line in [9].

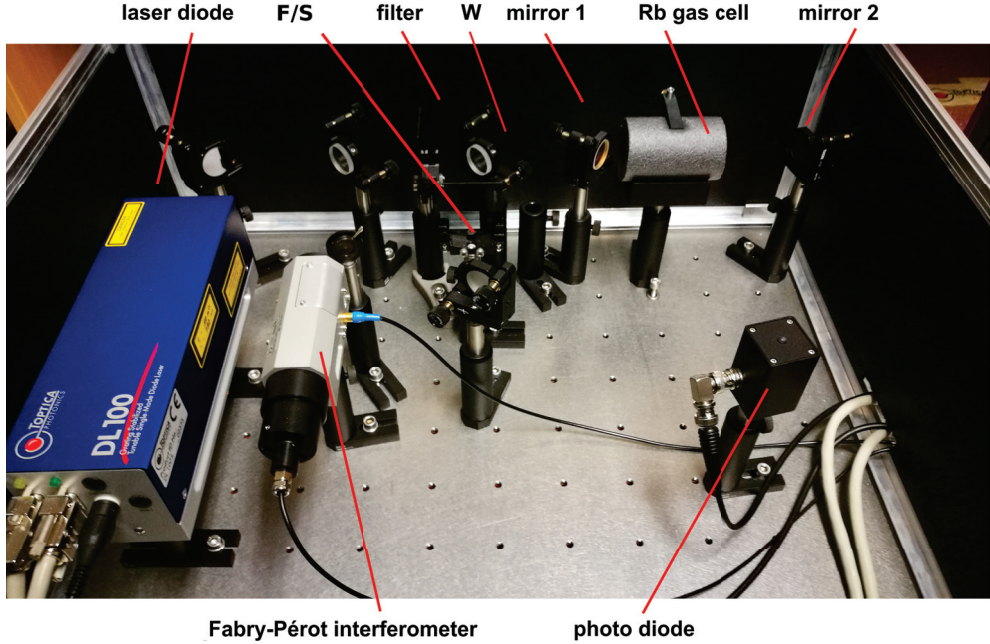


Figure 14: Experimental set-up with different optical elements.

6 Saturation spectroscopy

The set-up of this experiment is shown in figure 14. The laser light generated in the laser diode is directed by a first mirror onto a beam splitter. One part of the beam is attenuated by an adjustable aperture and coupled into the Fabry-Pérot interferometer. The second part of the beam is attenuated by a filter and reaches a second beam splitter. The portion passing through the beam splitter is the pump beam, i.e. it passes straight through the gas cell. The reflected portion (probe beam) is attenuated once more by a filter or an adjustable filter wheel and then guided by a mirror in the middle of the box onto mirror 2. From there it passes the gas cell anti-collinear with respect to the pump beam. The semi-transmissive mirror 1 serves to guide the probe beam to the photodiode (the photodetector), where its intensity is recorded. Two different spectra are measured: the transmission spectrum of the Fabry-Pérot interferometer and the absorption or saturation spectrum at the photodetector.

By blocking the beam path at point W , one can record pure absorption spectra; removing the blockage results in a saturation spectrum. In order to understand the beam trajectories, it is useful to let the supervisor block the beam at different locations and to watch the results on the computer at the same time.

A good description of the frequency stabilization procedure for a diode laser using the rubidium D_2 line can be found in [10].

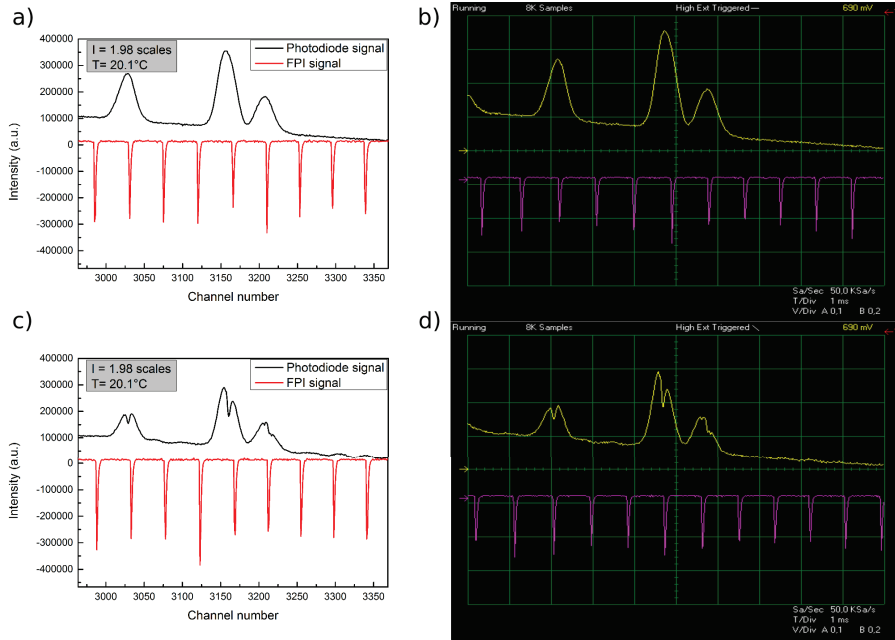


Figure 15: Representation of the raw data of an absorption (a), (b), or saturation spectrum (c), (d). From the characteristics of the FPI, the distances of the individual peaks and thus also the positions of the resonances can be determined.

7 Experimental procedure and list of tasks

Safety note: During all experiments one should wear laser goggles with a suitable wavelength range. Such goggles are found at the workplace. When adjusting the laser beam, you must never drop your eyes to the level of the beam path! Also, omit to place arms or hands into the beam path! For adjustments a converter card is provided whose non-active area serves as handle. Rubidium is extremely reactive when getting in contact with air. If the rubidium cell breaks during the experiment, cover the the rubidium cell with sand (found next to the box with the experimental set-up) and notify the supervisor. Contact with water is to be strictly avoided !! Don't take any risk here!

In this experiment, two data sets are recorded simultaneously: the intensity distribution measured by the photodiode and the FPI modes of the laser radiation. Simultaneous recording is used to adjust the laser to single-mode operation and the known spacing of the individual peaks allows for a quantitative evaluation of the measured data. A typical set of measurement is shown in figure 15. The spectra are acquired using the *EasyScopeII* software for DS1M12. The user interface is shown in figure 16. A detailed manual on the functions and operation of the software can be found at [11].

In the practical part of this lab experiment the following tasks have to be completed:



Figure 16: User interface of the EasyScope II for DS1M12 software with saturation spectrum (yellow) and FPI signal (purple).

Hints:

- Before switching on the device, read paragraph 4.3 "Power Up and Check of the Production and Quality Control Data Sheet" in the "Grating Stabilized Diode Laser Head Manual" which is provided on the desk.
 - When the device is switched on for the first time, the warning light I_{max} on the DTC110 module lights up shortly. This is normal, as long as lights off within a minute. It owes to the notable temperature difference between the environment and the laser diode at the beginning.
 - Before starting the experiment, the scan amplitude must be set to its maximum value by means of the rotary knob on the SC110 module. The scan varies the injection current around the set value. The wavelength tuning of the laser is realized by adjusting the external grating by means of a voltage ramp to the attached piezo.
1. Before starting the actual measurements, adjust the current and the temperature of the laser (in very small steps) so that the peaks on the display in the FPI spectrum are equidistant and of equal height. If this is the case, but no characteristic saturation spectrum can be detected, then you should shift the display using the slide cursor in the line below the display. Once a saturation spectrum has been detected and the FPI transmission spectrum has assumed the form described above, the measurements can be started.

In preparation. In the first part of the task, mirror 1 (see figure 14) should be adjusted by means of a servo in such a way that the signal on the photodiode becomes maximum. The servo changes the (in plane) angle between the mirror surface and the surface of the Rb gas cell. In particular, there is no vertical tilting! When adjusting a laser experiment, it must always be ensured that the beam is guided in one plane only to avoid dangerous scattered radiation. One should first familiarize with the effect of the servo on the mirror when the laser is off. Then close the box of the experimental set-up and make the adjustment by the absorption or saturation signal using the *EasyScopeII* software.

In preparation. The influence of collinearity between the pump and the probe laser beam will now be investigated. For this purpose, analogously to the first task mirror 2 is first moved by a certain distance by means of a servo. Then the mirror 1 is again adjusted so that the signal on the photodetector becomes maximum. The saturation spectra at different mirror settings are to be plotted and compared. Explain the resulting tendencies! Before carrying out the next part of the experiment, adjust the servos for maximum signal intensity on the photodiode.

2. Next, record multiple (seven to ten) spectra at different currents for five different temperatures between 19,8°C and 20,2°C. To adjust the temperature use the rotary knob on the DTC110 and to adjust the current the corresponding knob on the DCC110 module. The temperature can be read off the display window of the

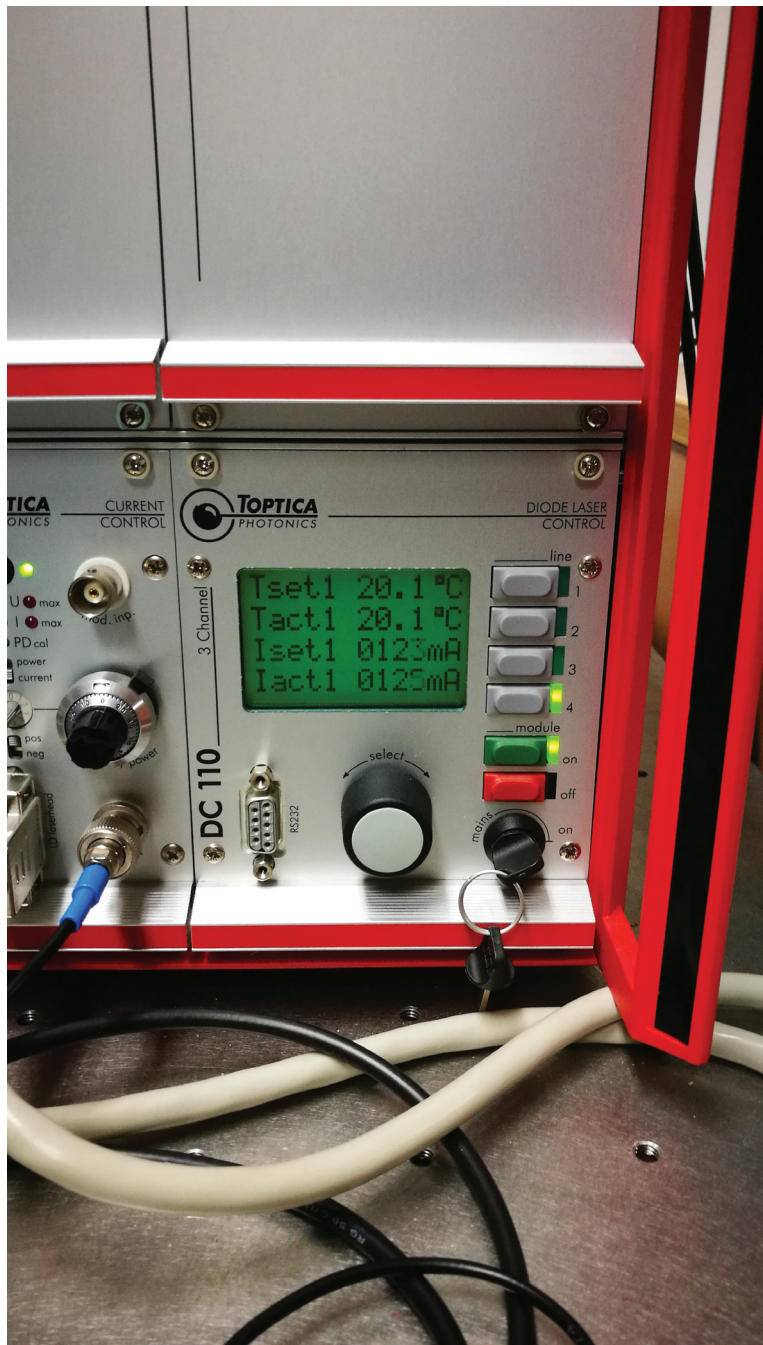


Figure 17: The display module on which the set and actual measurement parameters (temperature, current, voltage) can be controlled. Use the *module – off* and *module – on* buttons to turn the laser beam on or off. The key is used to switch on the entire device and should be turned last when switching off.

DC110 module. For the currents, it is sufficient to read off the numerical values on the associated rotary knob. However, if a mode jump occurs the actual current value is to be determined. For this purpose reduce the scan amplitude to 0 (rotary knob on the *SC110* module), since the injection function constantly changes the injection current. Then, the current can be read off from the display window. The thus obtained spectra are to be plotted and the trend described. How differ the spectra at different temperatures? What influence does the injection current have in the region between two mode jumps?

3. Now, instead of the filter plate with fixed attenuation, a filter wheel with filter gradient is placed at the position *F/S*. Before opening the test box, first turn off the laser using the red off button in the lower right corner of the *DC110* module. Absorption and saturation spectra at at least five different filter wheel settings are now to be recorded and compared with each other.
4. In the fourth part of the experiment absorption and saturation spectra at different temperatures and currents are to be recorded. Absorption spectra are recorded by interrupting the (pump) beam path at position *W* (see figure 14), e.g. by using the converter card.

Please read the relevant information in the device descriptions provided on the website in advance of the experiment. Among other things, the procedure to turn on the device is given. Other parameters than those described above must *not* be changed without contacting the supervisor in advance.

In addition to recording and displaying the spectra in the report, these should also be evaluated and labeled. Furthermore, the following tasks have to be completed:

1. Scale your measurement data using the FPI transmission peaks.
2. Determine the finesse of the FPI from the FPI transmission spectra.
3. Assign the visible peaks and lamb dips using appropriate literature (e.g. [12]) to the corresponding hyperfine structure transitions of the *D₂* line. Compare their distance and spectroscopic characteristics with literature values (e.g. in [3],[4],[13]).
4. Fit the peaks in the absorption spectrum with a suitable fitting function. Extract the characteristics of the individual peaks and compare them with literature values.

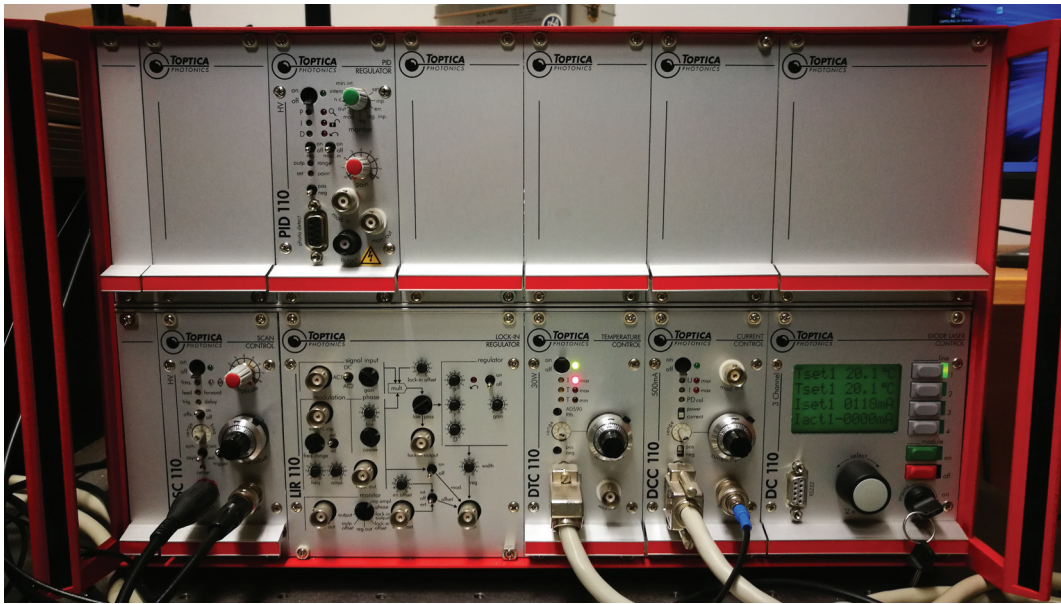


Figure 18: The control module of the photodiode, in which e.g. temperature and current setpoints can be adjusted. Before starting the experiment, the setting of the maximum values should be checked which are given in the corresponding manual.

References

- [1] Wolfgang Demtröder. *Laserspektroskopie 2*. Springer: Springer Spektrum, 2013. ISBN: 978-3-642-21446-2.
- [2] M. Ando T. Ida and H. Toraya. “Extended pseudo-Voigt function for approximating the Voigt profile”. In: *Journal of Applied Crystallography* 33 (2000), pp. 1311–1316.
- [3] Daniel A Steck. *Rubidium 87 D line data*. 2001.
- [4] Daniel A Steck. “Rubidium 85 D line data, Rubidium 87 D line data”. In: <http://steck.us/alkalidata> (2008).
- [5] Frank Thuselt. *Physik der Halbleiterbauelemente*. Vol. 1. 2005.
- [6] Marius Grundmann. *The Physics of Semiconductors*. Vol. 2. 2010.
- [7] Jan Bartl, Roman Fira, and Vlado Jacko. “Tuning of the laser diode”. In: *Measurement Science Review* 2.3 (2002).
- [8] Malvin Carl Teich and B Saleh. *Fundamentals of photonics*. Vol. 3. 1991.
- [9] J.L.Picque and S. Roizen. “Frequency-controlled cw tunable GaAs laser”. In: *Applied Physics Letters* 27.6 (1975), pp. 340–342. DOI: [10.1063/1.88468](https://doi.org/10.1063/1.88468).
- [10] Hidemi Tsuchida et al. “Frequency Stabilization of AlGaAs Semiconductor Laser Based on the 85 Rb-D 2 Line”. In: *Japanese Journal of Applied Physics* 21.9A (1982), p. L561.

- [11] 2006 USB-Instruments. *EasyScope II for DS1M12 "Stingray" - Help*.
- [12] A.M. Akulshin et al. “Power broadening of saturation absorption resonance on the D2 line of rubidium”. In: *Optics Communications* 77.4 (1990), pp. 295 –298. ISSN: 0030-4018. DOI: [http://dx.doi.org/10.1016/0030-4018\(90\)90094-A](http://dx.doi.org/10.1016/0030-4018(90)90094-A).
- [13] Shigeru Nakayama. “Theoretical Analysis of Rb and Cs D 2 Lines in Saturation Spectroscopy with Optical Pumping”. In: *Japanese Journal of Applied Physics* 23.7R (1984), p. 879.